UC Riverside

Title

Beyond Conventional Density Functional Theory: Advanced Quantum Dynamical Methods for Understanding Degradation of Per- and Polyfluoroalkyl Substances.

Permalink

Journal

Authors

Biswas, Sohag
Wong, Bryan

Publication Date

DOI

Peer reviewed

Beyond Conventional Density Functional Theory: Advanced Quantum Dynamical Methods for Understanding Degradation of Per- and Polyfluoroalkyl Substances

Sohag Biswas and Bryan M. Wong*

ACCESS | Metrics & More | Article Recommendations

ABSTRACT: Computational chemistry methods, such as density functional theory (DFT), have now become more common in environmental research, particularly for simulating the degradation of per- and polyfluoroalkyl substances (PFAS). However, the vast majority of PFAS computational studies have focused on conventional DFT approaches that only probe static, *time-independent* properties of PFAS near stationary points on the potential energy surface. To demonstrate the rich mechanistic information that can be obtained from *time-dependent* quantum dynamics calculations, we highlight recent studies using these advanced techniques for probing PFAS systems. We briefly discuss recent applications ranging from *ab initio* molecular dynamics to DFT-based metadynamics and real-time time-dependent DFT for probing PFAS degradation in various reactive environments. These quantum dynamical approaches provide critical mechanistic information that cannot be gleaned from conventional DFT calculations. We conclude with a perspective of promising research directions and recommend that these advanced quantum dynamics simulations be more widely used by the environmental research community to directly probe PFAS degradation dynamics and other environmental processes.

KEYWORDS: *per- and polyfluoroalkyl substances, PFAS, quantum dynamics, ab initio molecular dynamics, density functional theory*
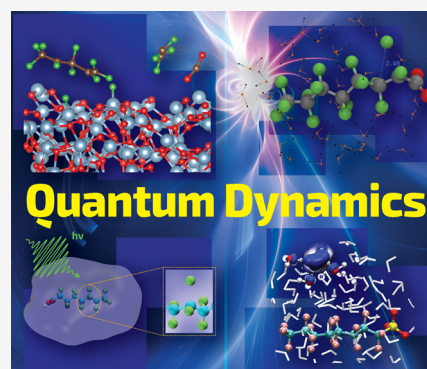
INTRODUCTION

Per- and polyfluoroalkyl substances (PFAS) comprise a group of manufactured chemical compounds used in a variety of consumer products, such as nonstick cookware,[1] stain-resistant fabrics, paint, and firefighting foams.[2] Mitigating PFAS compounds has attracted recent interest since they persist in the environment and do not break down quickly, gaining them the nickname "forever chemicals".[3] In addition to being detected in soil and water sources around the world,[3−7] PFAS can bioaccumulate in the food chain and persist in animal and human tissue over time.[8−11] Most importantly, exposure to PFAS can have damaging health effects, including liver damage, thyroid disease, decreased fertility, and certain cancers.[12] Because of these deleterious effects, several computational efforts have focused on understanding PFAS reactivity to predict new chemical approaches for removing these pollutants from the environment.[13−20]

Among the various computational chemistry methods used to investigate PFAS reactivity, density functional theory (DFT) continues to be the most popular approach due to its reasonable balance between accuracy and computational cost. However, the vast majority of DFT studies on PFAS have focused on conventional computational approaches that probe static *time-independent* properties only near stationary points on the PFAS potential energy surface. More specifically, static

DFT studies of PFAS provide a single snapshot of equilibrium electronic structures, total energies, and electronic properties for a fixed configuration of atoms. In contrast, quantum dynamics simulations utilize a time-dependent approach (by integrating the quantum mechanical equations of motion) to track the evolution of atomic positions and electronic structure over time, capturing dynamic phenomena such as time-resolved chemical reactions, thermal effects, and electronic-excited states. In short, static DFT calculations of PFAS are restricted to time-independent equilibrium properties, whereas quantum dynamics approaches inherently capture time-dependent nonequilibrium phenomena.

In this Perspective, we focus on a variety of quantum dynamic approaches for probing PFAS degradation in various reactive environments. While there have been several studies using DFT to explore PFAS mechanisms, there have been fewer computational studies examining dynamical (i.e.,
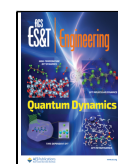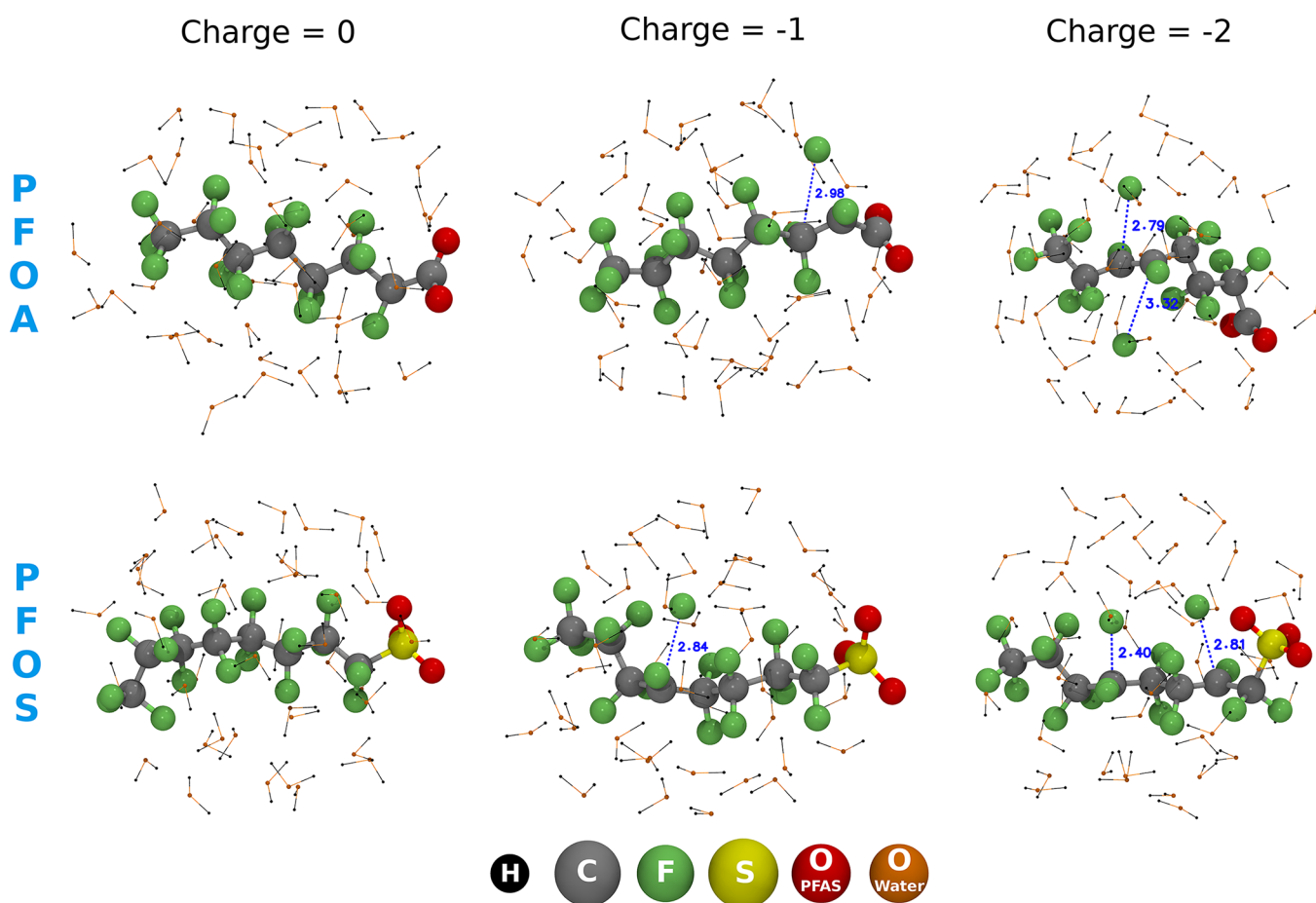
Figure 1. Geometries of solvated PFOA (top panel) and PFOS (bottom panel) anions after 1 ps of NVE simulations with 0 (left), 1 (middle), and 2 (right) excess electrons. PFOA and PFOS lose their acidic proton to the surrounding water molecules during the simulation and are found in their anionic forms. Both PFOA and PFOS are stable in neutral environments, whereas defluorination rapidly occurs in the presence of 1 and 2 excess electrons. Reprinted in part with permission from ref 16. Copyright 2020, Royal Society of Chemistry.

explicitly time-dependent) processes for PFAS. The purpose of this short perspective is to provide an update on recent developments in advanced quantum dynamical methods for probing/understanding PFAS degradation mechanisms. We present examples of *ab initio* molecular dynamics, DFT-based metadynamics, high-temperature reactivity studies, and real-time time-dependent DFT approaches for probing the intrinsically dynamic nature of the PFAS degradation process. These approaches directly provide time-resolved dynamical, temperature-, and light-induced effects that cannot be gleaned from conventional DFT calculations. We finally conclude with a perspective of promising research directions for probing PFAS degradation dynamics and other environmental processes in this vibrant research area.

■ *AB INITIO* MOLECULAR DYNAMICS: PFAS DEGRADATION DYNAMICS IN CHARGED ENVIRONMENTS

One of the most effective methods for PFAS remediation is the use of advanced reduction processes (ARPs) to chemically degrade these contaminants. In ARPs, strongly reducing species, such as hydrated electrons (e_{aq}^-), hydrogen radicals (H•), or radicals from a catalyst, are harnessed to induce C−F bond cleavage in PFAS. In the context of computational studies on ARPs, the vast majority of DFT approaches on PFAS degradation have been limited to static calculations that

do not give direct information on defluorination time scales or kinetics.[21−24] To provide mechanistic insight into time-resolved PFAS degradation dynamics in strongly reducing environments, our group carried out the first *ab initio* molecular dynamics (AIMD) simulations of perfluoroocata-noic acid (PFOA) and perfluorooctanesulfonic acid (PFOS) in electrostatically charged aqueous environments.[25] In these simulations, each PFAS molecule was solvated with 43 explicit water molecules in the presence of excess charges/electrons using a self-interaction corrected PBE[26] functional. Figure 1 depicts representative snapshots of solvated PFOA and PFOS after 1 ps of NVE (constant Number, Volume, and Energy) simulations. The first column in Figure 1 shows that these pollutants are stable in neutral aqueous environments, in agreement with experiment. The middle and right columns in Figure 1 depict AIMD results with −1 and −2 charges for both PFOA and PFOS. These snapshots show that excess electrons dissociate the strongest C−F bonds in PFAS at ultrafast time scales (<100 fs). Our AIMD simulations showed that the number of dissociated C−F bonds is proportional to the number of additional electrons in the simulation box. In addition, the defluorination of PFAS in the presence of two excess electrons leads to the trans-elimination of F atoms, forming an intermediate with an alkene-type C=C bond, which is a crucial step in the PFAS degradation process. In addition, these simulations also showed that the formation of
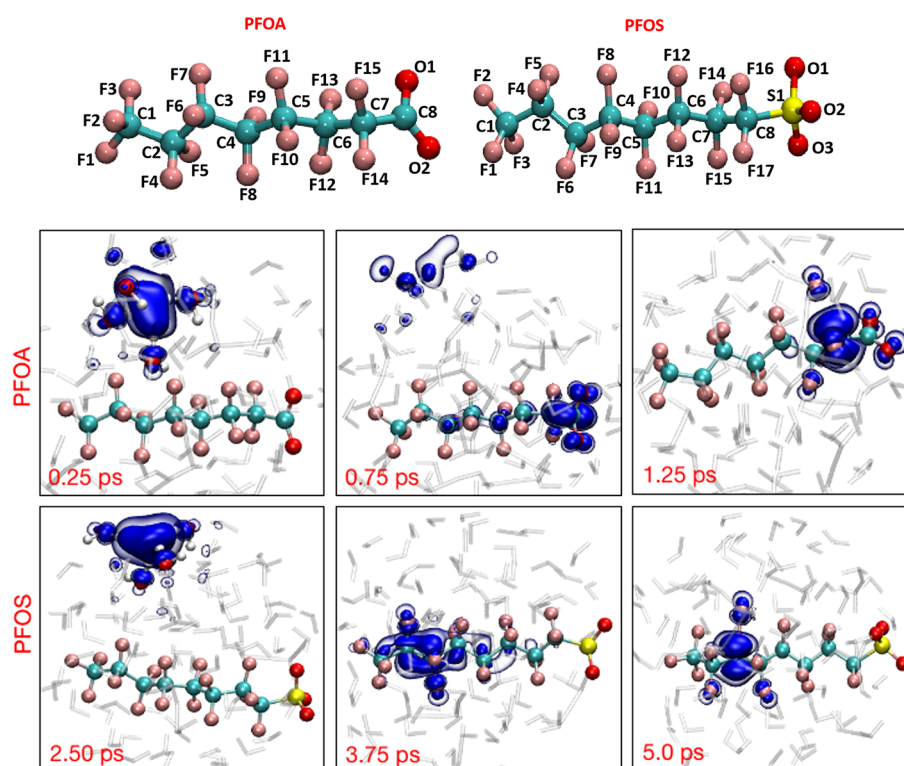
Figure 2. (Top panels) Chemical structure and atom numbering scheme of the PFOA and PFOS anions. Time-resolved evolution of the spin density of the hydrated electron for representative trajectories of PFOA (middle panels) and PFOS (bottom panels). Reprinted in part with permission under a Creative Commons BY-NC-ND 4.0 License from ref 19. Copyright 2022, American Chemical Society.

an H−F molecule is a possible outcome of the BOMD simulations. Taken together, these AIMD calculations enabled new time-resolved quantum calculations of the degradation process and provided the first real-time picture of PFAS degradation in charged environments.[16]

DFT-BASED METADYNAMICS: PFAS DEGRADATION DYNAMICS VIA HYDRATED ELECTRONS

While the previous section discussed PFAS degradation dynamics in the presence of excess charges, it is important to note that simply adding an extra electron to an *ab initio* molecular dynamics simulation *does not* accurately simulate hydrated electrons used in ARP experiments. This discrepancy arises because the surrounding water molecules around that excess charge do not polarize the extra electron, which produces unrealistic configurations of the hydrated electron compared to experiments. A hydrated electron can only be formed when the excess electron has lost sufficient energy to create a metastable localized species bound with water.[27,28]

To simulate the dynamics of a hydrated electron, we used both AIMD and DFT-based metadynamics to probe its reactivity with PFOA and PFOS.[19] Figure 2 shows time-resolved spin-density dynamics of the hydrated electron and the subsequent C−F defluorination of PFOA/PFOS in the presence of 81 explicit water molecules. Further details on how we initialized the system with a hydrated electron are given in ref 19. Most notably, the defluorination mechanism of PFAS via a hydrated electron differs from that of an excess electron. When the system is simulated with an excess electron, the spin density of the excess electron artificially spreads out over the entire PFAS molecule. The excess electron subsequently

shrinks and further polarizes the PFAS molecule, until the spin density slowly accumulates at the dissociation site. In contrast, the spin density of a hydrated electron is primarily localized in a cavity and stabilized by approximately four water molecules with their O−H bonds pointing toward the center of the cavity. Our AIMD calculations showed that the spin density of the hydrated electron transfers from the cavity to the PFAS molecule as the simulation proceeds. The spin density accumulates at the dissociation site, and defluorination subsequently occurs. In solvated PFOA, C−F bond dissociation occurs within one picosecond. For PFOS, the time scales vary from femtoseconds to a few picoseconds. This disparity in time scales arises from the hydrated-electron cavity being more compact and strongly bound with water molecules, making it less reactive toward the PFOS molecule. For these cases, the hydrated electron preferentially attacks either the C3 or C4 sites (see Figure 2).

To provide deeper insight into the free-energy dynamics for the various C−F bond cleavages initiated by the hydrated electron, our group carried out well-tempered metadynamics simulations.[29] Well-tempered metadynamics is an advanced molecular dynamics technique that can be used to study rare events and free-energy landscapes.[30−33] Figure 3 summarizes the activation energies for C−F bond dissociation in solvated PFOA and PFOS using a hydrated electron. The average free energy barrier values for the C−F bond dissociation from these independent trajectories are 2.70 and 8.16 kJ/mol for PFOA and PFOS, respectively. Our metadynamics calculations showed that the average free activation barrier for C−F bond dissociation in PFOS is three times larger than that of PFOA. Additional statistical analyses (such as radial distribution calculations) were carried out in ref 19, which showed that
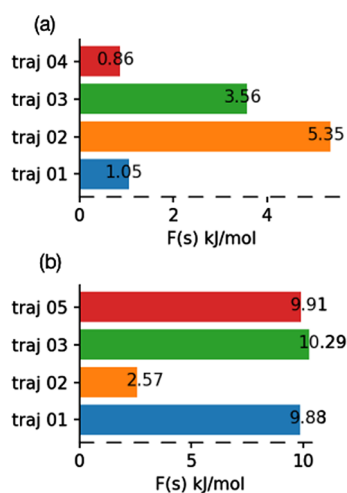
Figure 3. Free energy activation barrier values for C−F bond dissociation via hydrated electrons in solvated (a) PFOA and (b) PFOS. Reprinted in part with permission under a Creative Commons BY-NC-ND 4.0 License from ref 19. Copyright 2022, American Chemical Society.

the hydrated electron has a more rigid/compact solvation shell, making it less reactive toward PFOS, resulting in slower defluorination. In both cases, the free energy activation barriers for PFOS and PFOA fall below the diffusion-controlled limit, which indicates that the degradation process is independent of the overall chemical rate constant.[19,34] The most salient point of these metadynamics calculations is that all of the C−F

bonds in PFAS have a high probability of dissociating in the presence of hydrated electrons. This phenomenon arises since PFAS degradation via hydrated electrons is a kinetic/statistical process and not a thermodynamic one. In other words, even though certain C−F bonds are thermodynamically more reactive, all of the other C−F bonds also have a high probability (whose statistics can be explored by AIMD simulations) to dissociate. Taken together, these DFT-based metadynamics simulations were the first *ab initio* dynamics study of PFAS degradation via hydrated electrons, a configuration that had not been correctly considered in previous computational studies up to this point.[19]

AB INITIO MOLECULAR DYNAMICS AT HIGH TEMPERATURES: PFAS DEGRADATION DYNAMICS ON SURFACES

In addition to ARPs in aqueous environments discussed previously, there has also been recent work on harnessing solid surfaces for the enhanced degradation of PFAS contaminants. Specifically, metal-oxide surfaces with *d*-block metal atoms have emerged as potential substrates due to their high heterogeneity and diverse coordination/bonding motifs, which can accelerate PFAS degradation.[18] Because of the complicated nature of high-temperature experiments, there is currently a lack of knowledge of the mechanisms involved in PFAS degradation on material surfaces. To bridge this knowledge gap, our group conducted the first AIMD study on PFOA degradation dynamics on various γ-Al$_2$O$_3$ surfaces over a wide range of temperatures. γ-Al$_2$O$_3$ exhibits significant surface heterogeneity, with Al atoms displaying tri-, tetra-, and
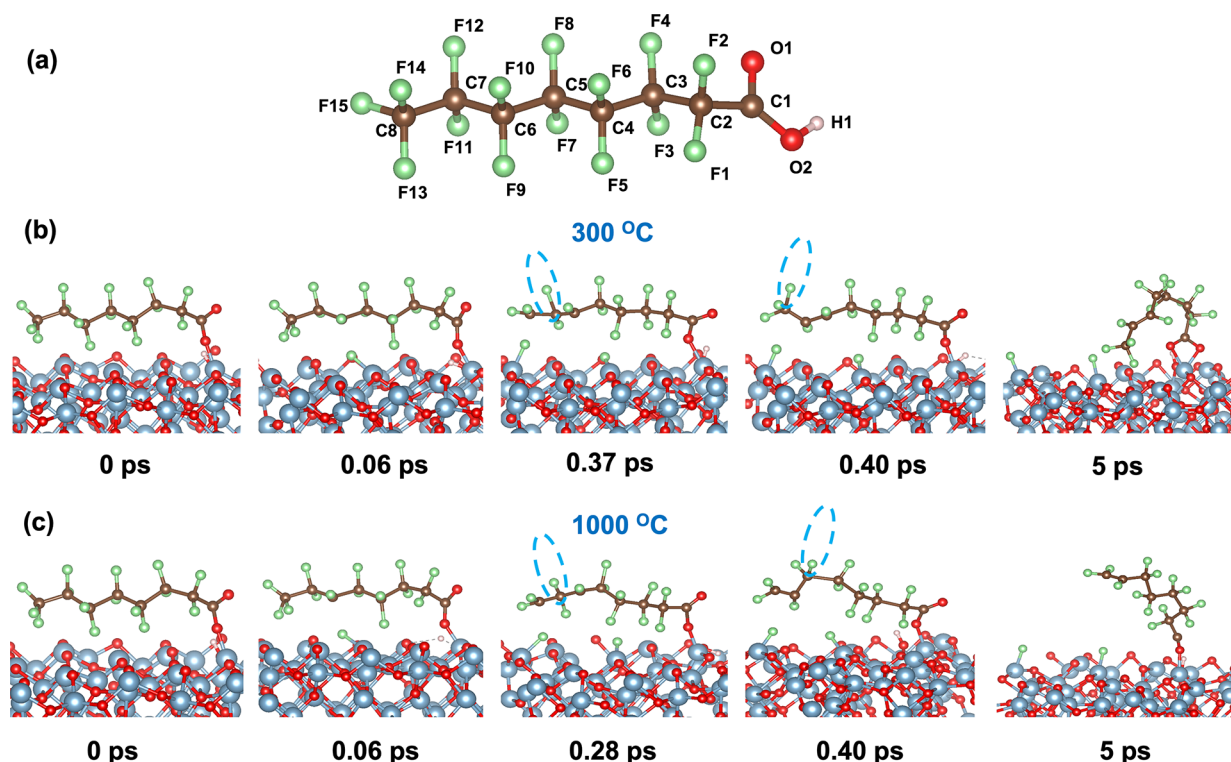

Figure 4. (a) Atom numbering scheme of the PFOA molecule. Time-resolved snapshots depicting dissociation of various C−F bonds of PFOA on the γ-Al$_2$O$_3$ (100) surface with an oxygen-vacancy defect at (b) 300 and (c) 1000 °C, respectively. The dashed oval in panel (a) shows the migration of the F atom from the C7 (0.37 ps) to the C8 position (0.40 ps), whereas the dashed oval in panel (b) indicates the migration of the F atom from the C7 (0.28 ps) to the C6 position (0.40 ps). Reprinted in part with permission under a Creative Commons BY-NC-ND 4.0 License from ref 18. Copyright 2023, American Chemical Society.
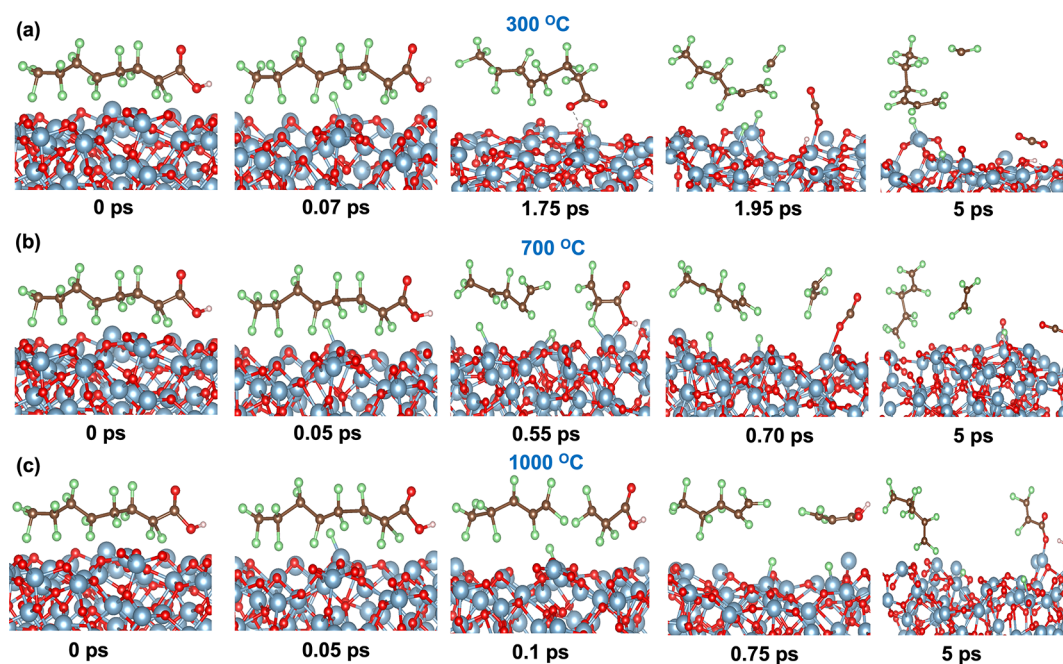
Figure 5. Time-resolved snapshots of representative trajectories illustrate degradation of PFOA on the γ-Al$_2$O$_3$ (110) surface. Panels (a), (b), and (c) depict degradation mechanisms at 300, 700, and 1000 °C, respectively. Reprinted in part with permission under a Creative Commons BY-NC-ND 4.0 License from ref 18. Copyright 2023, American Chemical Society.

pentacoordination, which enhances its reactivity as shown in previous studies.[35,36] To predict PFOA degradation dynamics at elevated temperatures, we carried out AIMD calculations on the (100) and (110) surfaces of γ-Al$_2$O$_3$ by taking into account possible surface defects.

Our AIMD simulations showed that PFOA defluorination occurs extremely quickly (<100 fs) when an oxygen vacancy is present on the (100) surface of γ-Al$_2$O$_3$. Figure 4 shows that the initial step in PFOA defluorination (at all temperatures) is C−F bond cleavage at the C6 position accompanied by the creation of an Al−F bond. Subsequent steps involve the dissociation of other C−F bonds when an Al(III) atom on the γ-Al$_2$O$_3$ (100) surface abstracts an F atom from the C8 position. The F atom at the C7 center then migrates toward either the C8 (at 300 °C) or C6 center (at 600 °C). At the end of the AIMD simulations, a C═C bond is formed, and the PFOA molecule becomes chemically bonded to the γ-Al$_2$O$_3$ surface. We observed similar degradation mechanisms at 700 and 1200 °C (figures not shown). Our AIMD calculations further showed that the surface oxygen vacancy enables dissociative adsorption and defluorination of PFOA since the oxygen vacancy transforms Al(IV) atoms on the surface from a tetrahedral coordination to a tricoordinated Al(III) center. This transformation increases the Lewis acidic character of Al(III) and results in a stronger interaction between the F atoms of PFOA and Al(III) atoms on the surface, thereby facilitating the dissociation of C−F bonds. Static DFT calculations, which do not include thermal effects, have previously predicted the CF$_2$ unit at the α-position adjacent to the −COOH group to be more reactive due to inductive effects of the headgroup.[20] However, our AIMD simulations, which explicitly account for thermal effects, indicated that delfuorination occurs primarily near the terminal end of PFOA due to the proximity of F atoms to Al(III) centers on the γ-Al$_2$O$_3$ (100) surface.

Figure 5 depicts the degradation mechanisms of PFOA on the γ-Al$_2$O$_3$ (110) surface at various temperatures. It is worth noting that the (110) surface exclusively contains Al(III) centers (which are more Lewis acidic than Al(IV)), whereas the (100) surface has only Al(IV) and Al(V) centers. The degradation of PFOA on the pristine (110) surface differs significantly from that on the (100) surface with an oxygen vacancy. Dissociation of the C5−F7 bond and cleavage of the C−COO and C−C bonds in PFOA occurred rapidly on the pristine (110) surface at temperatures above or equal to 300 °C. At 300 °C, a second defluorination occurs at the C4 center in tandem with dissociation of the C1−C2 and C2−C3 bonds. During our AIMD simulations, we noted the formation of a bond between Al(III) and one of the oxygen atoms in PFOA. Interestingly, the time scales for Al−O bond formation, C−F defluorination, and dissociation of C−C bonds were similar, suggesting that COO···Al and Al···F interactions activate C−C and C−F bonds. We observed the same PFOA degradation mechanism on the γ-Al$_2$O$_3$ (110) surface at 700 °C, except for dissociation of the C1−C2 and C3−C4 bonds. However, at 1000 and 1200 °C (figure not shown), only the C3−C4 bond dissociated, and the second defluorination occurred at the C2 center. Hence, the AIMD simulations provide a significant mechanistic understanding of PFOA degradation by considering the impact of temperature (not considered in conventional static DFT calculations) and atomic-level surface details, which are necessary for the efficient degradation of these PFOA contaminants. Taken together, these quantum dynamics simulations emphasize the importance of surface defects, crystallographic surface, and high temperatures (which static DFT calculations do not capture) for efficient PFOA degradation. Furthermore, these AIMD calculations provide detailed mechanistic information for prescreening suitable surfaces and temperatures to guide experimental efforts for remediating PFAS and other chemical contaminants.
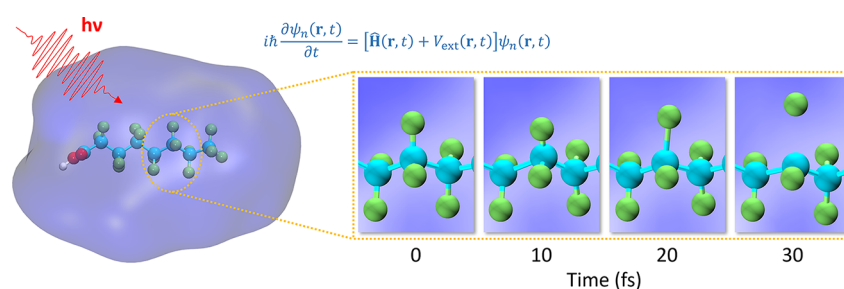
Figure 6. (a) PFOA molecule (explicit solvent not shown for clarity) with an applied optical pulse. (b) Dissociation of a C−F bond as a function of time obtained from propagation of the time-dependent Kohn−Sham equations. Reprinted in part with permission under a Creative Commons BY-NC-ND 4.0 License from ref 39. Copyright 2023, Elsevier.
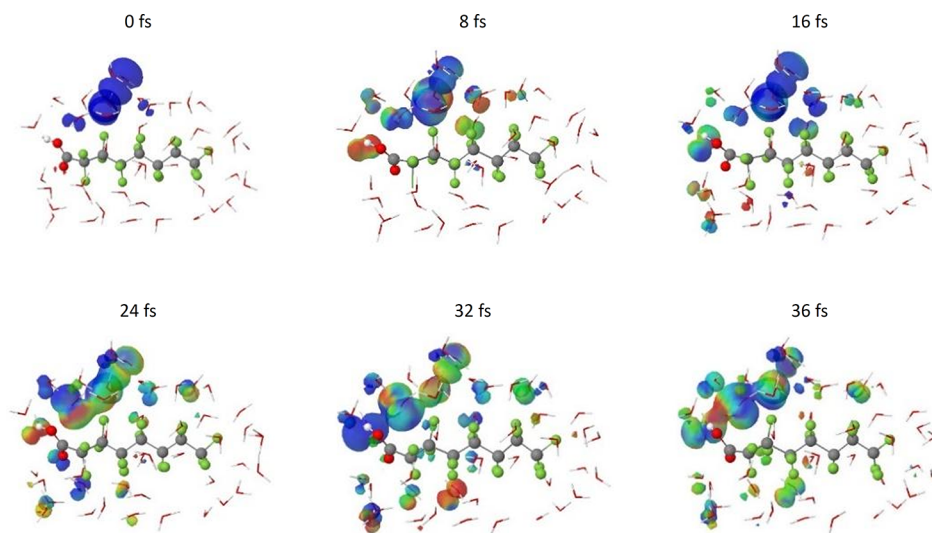

Figure 7. Evolution of the highest occupied molecular orbital of PFOA surrounded by 43 H_2O molecules as a function of time. As time progresses, charge dynamically transfers from the water to an antibonding orbital on PFOA. The C−F bond begins to subsequently destabilize and dissociate as it continues to vibrate dynamically. The positively charged hole remaining in the solvent arising from the aforementioned charge-transfer excitation becomes stabilized by the surrounding water molecules. Reprinted in part with permission Creative Commons BY 4.0 License from ref 17. Copyright 2022, Elsevier.

REAL-TIME TIME-DEPENDENT DFT: PHOTO-INDUCED PFAS DEGRADATION DYNAMICS

In this final section, we highlight recent work using advanced excited-state quantum dynamics simulations for understanding photoinduced degradation of PFAS. While the previous sections focused on PFAS degradation dynamics on the electronic *ground state*, computational studies on electronic *excited-state* dynamics of photoinduced degradation are even more scarce. This disparity arises from the difficulty and complexity of calculating the excited-state quantum dynamics of large chemical systems. In particular, most DFT studies on PFAS reactivity have focused on ground-state reactions,[16,19] "after the fact" when the light-induced process has already transpired. Although conventional DFT methods can examine local minima and transition states in ground-state systems, they cannot capture excited-state electron dynamics, which are essential for describing photocatalytic reactions in PFAS. Our group conducted the first real-time time-dependent density functional theory (RT-TDDFT) study on electronic-excited PFAS dynamics under the influence of external electromagnetic fields to gain a deeper understanding of these processes.[17] The RT-TDDFT approach[37,38] goes beyond traditional ground-state DFT methods to explore excited-

state dynamics, making it suitable for investigating photoinduced mechanisms and achieving a fundamental understanding of these electronic-excited PFAS degradation processes.

To shed mechanistic insight into these photoinduced processes, we implemented custom optical pulses in the GPAW software package[40] to execute large-scale RT-TDDFT simulations of PFAS/PFOS degradation dynamics. The initial configuration for our excited-state Ehrenfest dynamics was a PFOA/PFOS molecule surrounded by 43 explicit water molecules, and we monitored the atomic positions at each time step as the entire system was computationally irradiated with an external electromagnetic pulse. In a computational tour de force, the time-dependent Kohn−Sham equations were propagated to probe the photoinduced, excited-state dynamics responsible for initiating the defluorination process. Figure 6 depicts the irradiated PFOA molecule and selected snapshots of various C−F bonds as a function of time obtained from the RT-TDDFT calculations. Irradiation with an electromagnetic pulse drives the entire system to various electronic-excited states, which causes various C−F bonds in the PFOA molecule to oscillate and subsequently dissociate after 20 fs.

To gain additional mechanistic insight into these excited-state processes, we further analyzed the time-dependent

Kohn−Sham orbitals in Figure 7. Our RT-TDDFT results showed that the highest occupied molecular orbital (HOMO) is initially localized on the surrounding water molecules. Between 8 and 16 fs, the HOMO starts to delocalize onto the PFOA molecule, accompanied by a charge transfer from the surrounding water molecules to PFOA. The additional charge occupies the previously unoccupied $3s_F$ and $2p_C$ atomic orbitals on PFOA, which have a strong σ^* antibonding nature. Once these previously empty orbitals become occupied, a dissociative electron attachment (DEA) process occurs: the C−F bond destabilizes and elongates (since the HOMO now has an antibonding character) until it irreversibly dissociates. Filho et al. also carried out computational studies on excited-state decomposition of PFOA and PFOS in an effective continuum solvation model using linear-response TDDFT (LR-TDDFT) calculations.[41] In contrast to the RT-TDDFT formalism, LR-TDDFT is a frequency-domain solution of the time-dependent Kohn−Sham equations and is limited to small external perturbations that do not destroy the electronic ground state of the system. The LR-TDDFT calculations by Filho et al. showed dissociation of the SO_3^- group from the PFOS molecule with no significant changes in the molecular backbone composed of C−C and C−F bonds. For the PFOA molecule, the LR-TDDFT calculations showed that the COO^- group remained bonded to the molecular backbone, with the C−F bonds remaining intact. These results show different degradation mechanisms than our RT-TDDFT calculations since, as mentioned previously, LR-TDDFT calculations are a frequency-domain solution of the time-dependent Kohn−Sham equations in a perturbative regime. In contrast, the time-dependent nature of the RT-TDDFT formalism allows simulations with different field strengths/intensities and frequencies beyond the perturbative regime, which allows us to understand the effects of these parameters on the degradation process. It is worth mentioning that these excited-state RT-TDDFT calculations are much more computationally expensive than conventional ground-state DFT calculations. Specifically, these calculations required more than 570,000 high-performance computing (HPC) hours,[42] which was recently recognized with an HPCWire 2022 Editors' Choice Award for "Best Use of HPC in Response to Societal Plights."[43]

ENVIRONMENTAL IMPLICATIONS

The quantum dynamics simulations discussed in this Perspective have several significant environmental implications for PFAS remediation efforts. For example, the AIMD simulations highlight the statistical nature of the PFAS degradation dynamics. While specific C−F bonds may have a greater thermodynamic reactivity (as predicted by static DFT calculations), our AIMD simulations indicate that other C−F bonds in PFAS also have a high probability of dissociation. As a result, future research on remediation efforts should focus on minimizing the contact distance between PFAS molecules and reactive materials rather than solely targeting the thermodynamically weakest C−F bond.

In addition, the DFT-based metadynamics calculations provide clear evidence that PFAS degradation with hydrated electrons is a diffusion-limited process. To enhance the experimental efficiency of this process, one should minimize the distance that the hydrated electrons need to diffuse to reach the PFAS contaminant. One practical approach is to directly adsorb PFAS molecules onto an electrified surface or electron-rich material, which would reduce the diffusion distance that the generated hydrated electrons must traverse to dissociate PFAS.

Finally, the high-temperature AIMD and RT-TDDFT calculations highlight the usefulness of these approaches to systematically understand the effects of external conditions (i.e., temperature or electromagnetic fields) on the PFAS degradation process. In particular, these quantum dynamics calculations can be used to systematically prescreen the experimental conditions required to efficiently remediate these contaminants. Since these predictive calculations are inherently more time and cost efficient than trial-and-error experimentation, they enable a rational approach to guide experimental efforts in remediating PFAS contaminants.

CONCLUSION, CHALLENGES, AND FUTURE DIRECTIONS

In this Perspective, we have provided a brief overview of advanced quantum methods, including *ab initio* molecular dynamics, DFT-based metadynamics, high-temperature reactivity studies, and real-time time-dependent DFT for probing PFAS degradation in various reactive environments. The common thread in all these methods is their use of time-dependent quantum approaches to probe the intrinsically dynamic nature of the PFAS degradation process. Because of their time-dependent nature, all of these advanced dynamics calculations go beyond conventional, static (time-independent) DFT approaches commonly used to study environmental contaminants. Most notably, these approaches directly provide time-resolved dynamical, temperature-, and light-induced effects that cannot be gleaned from conventional DFT calculations. Harnessing these advanced quantum dynamics approaches allows us to gain insight into degradation kinetics, time-resolved reaction mechanisms, and experimental conditions that are crucial for assessing the efficacy of different PFAS degradation methods. Overall, these approaches can lead to a more comprehensive understanding of PFAS degradation that can be leveraged to develop more effective and sustainable remediation methods.

Looking forward, key issues that still need to be addressed are the accuracy and high computational expense associated with these advanced quantum dynamical approaches. For example, both the ground-state AIMD and excited-state RT-TDDFT simulations discussed in this Perspective can be routinely used only for relatively small systems. Moreover, PFAS degradation processes typically involve heterogeneous systems with complex interfaces and solvent interactions, which require larger system sizes to accurately represent the experimental environmental conditions. Consequently, extending both the length and time scales of these calculations would allow more realistic simulations that capture the spatial and temporal dynamics probed in PFAS degradation experiments. Progress on both these fronts is currently being tackled in our research group using excited-state semiempirical methods[44−47] and advanced hardware accelerators[48−51] to simulate large systems that cannot be easily obtained with conventional DFT. As algorithmic developments and computational resources improve, we recommend that these advanced quantum dynamics simulations be more widely used by the environmental research community to directly probe PFAS degradation dynamics and other environmental processes.

■ AUTHOR INFORMATION

Corresponding Author

Bryan M. Wong − Materials Science & Engineering Program, Department of Chemistry, and Department of Physics & Astronomy, University of California-Riverside, Riverside, California 92521, United States; ● orcid.org/0000-0002-3477-8043; Email: bryan.wong@ucr.edu

Author

Sohag Biswas − Materials Science & Engineering Program, Department of Chemistry, and Department of Physics & Astronomy, University of California-Riverside, Riverside, California 92521, United States

Complete contact information is available at:
https://pubs.acs.org/10.1021/acsestengg.3c00216

Author Contributions

CRediT: **Sohag Biswas** conceptualization, data curation, formal analysis, investigation, methodology, validation, visualization, writing-original draft, writing-review & editing; **Bryan M. Wong** conceptualization, formal analysis, funding acquisition, investigation, methodology, project administration, resources, supervision, writing-original draft, writing-review & editing.

Notes

The authors declare no competing financial interest.

■ REFERENCES

(1) Sajid, M.; Ilyas, M. PTFE-coated non-stick cookware and toxicity concerns: a perspective. *Environ. Sci. Pollut. Res.* **2017**, *24*, 23436−23440.

(2) Guelfo, J. L.; Adamson, D. T. Evaluation of a national data set for insights into sources, composition, and concentrations of per- and polyfluoroalkyl substances (PFASs) in U.S. drinking water. *Environ. Pollut.* **2018**, *236*, 505−513.

(3) Liu, F.; Guan, X.; Xiao, F. Photodegradation of per- and polyfluoroalkyl substances in water: A review of fundamentals and applications. *J. Hazard. Mater.* **2022**, *439*, No. 129580.

(4) Davis, K. L.; Aucoin, M. D.; Larsen, B. S.; Kaiser, M. A.; Hartten, A. S. Transport of ammonium perfluorooctanoate in environmental media near a fluoropolymer manufacturing facility. *Chemosphere* **2007**, *67*, 2011−2019.

(5) Lindstrom, A. B.; Strynar, M. J.; Delinsky, A. D.; Nakayama, S. F.; McMillan, L.; Libelo, E. L.; Neill, M.; Thomas, L. Application of WWTP biosolids and resulting perfluorinated compound contamination of surface and well water in Decatur, Alabama, USA. *Environ. Sci. Technol.* **2011**, *45*, 8015−8021.

(6) McDonough, C. A.; Choyke, S.; Barton, K. E.; Mass, S.; Starling, A. P.; Adgate, J. L.; Higgins, C. P. Unsaturated PFOS and other PFASs in human serum and drinking water from an AFFF-impacted community. *Environ. Sci. Technol.* **2021**, *55*, 8139−8148.

(7) Xiao, F.; Simcik, M. F.; Gulliver, J. S. Mechanisms for removal of perfluorooctane sulfonate (PFOS) and perfluorooctanoate (PFOA) from drinking water by conventional and enhanced coagulation. *Water Res.* **2013**, *47*, 49−56.

(8) Lau, C.; Thibodeaux, J. R.; Hanson, R. G.; Narotsky, M. G.; Rogers, J. M.; Lindstrom, A. B.; Strynar, M. J. Effects of perfluorooctanoic acid exposure during pregnancy in the mouse. *Toxicol. Sci.* **2006**, *90*, 510−518.

(9) Brown, J. B.; Conder, J. M.; Arblaster, J. A.; Higgins, C. P. Assessing human health risks from per- and polyfluoroalkyl substance (PFAS)-impacted vegetable consumption: a tiered modeling approach. *Environ. Sci. Technol.* **2020**, *54*, 15202−15214.

(10) Beach, S. A.; Newsted, J. L.; Coady, K.; Giesy, J. P. *Reviews of Environmental Contamination and Toxicology: Continuation of Residue Reviews*; Springer New York: New York, 2006; pp 133−174.

(11) Sznajder-Katarzyńska, K.; Surma, M.; Cieślik, I. A review of perfluoroalkyl acids (PFAAs) in terms of sources, applications, human exposure, dietary intake, toxicity, legal regulation, and methods of determination. *J. Chem.* **2019**, *2019*, 1.

(12) *C-8 Medical Monitoring Program*. http://www.c-8medicalmonitoringprogram.com/ (accessed April 18, 2023).

(13) Raza, A.; Bardhan, S.; Xu, L.; Yamijala, S. S. R. K. C.; Lian, C.; Kwon, H.; Wong, B. M. A machine learning approach for predicting defluorination of per- and polyfluoroalkyl substances (PFAS) for their efficient treatment and removal. *Environ. Sci. Technol. Lett.* **2019**, *6*, 624−629.

(14) Zhong, S.; Zhang, K.; Bagheri, M.; Burken, J. G.; Gu, A.; Li, B.; Ma, X.; Marrone, B. L.; Ren, Z. J.; Schrier, J.; Shi, W.; Tan, H.; Wang, T.; Wang, X.; Wong, B. M.; Xiao, X.; Yu, X.; Zhu, J.-J.; Zhang, H. Machine learning: New ideas and tools in environmental science and engineering. *Environ. Sci. Technol.* **2021**, *55*, 12741−12754.

(15) Kwon, H.; Ali, Z. A.; Wong, B. M. Harnessing semi-supervised machine learning to automatically predict bioactivities of per- and polyfluoroalkyl substances (PFASs). *Environ. Sci. Technol. Lett.* **2022**, DOI: 10.1021/acs.estlett.2c00530.

(16) Yamijala, S. S. R. K. C.; Shinde, R.; Wong, B. M. Real-time degradation dynamics of hydrated per- and polyfluoroalkyl substances (PFASs) in the presence of excess electrons. *Phys. Chem. Chem. Phys.* **2020**, *22*, 6804−6808.

(17) Yamijala, S. S.; Shinde, R.; Hanasaki, K.; Ali, Z. A.; Wong, B. M. Photo-induced degradation of PFASs: Excited-state mechanisms from real-time time-dependent density functional theory. *J. Hazard. Mater.* **2022**, *423*, No. 127026.

(18) Biswas, S.; Wong, B. M. Degradation of perfluorooctanoic acid on aluminum oxide surfaces: New mechanisms from ab initio molecular dynamics simulations. *Environ. Sci. Technol.* **2023**, *57*, 6695−6702.

(19) Biswas, S.; Yamijala, S. S. R. K. C.; Wong, B. M. Degradation of per- and polyfluoroalkyl substances with hydrated electrons: A new mechanism from first-principles calculations. *Environ. Sci. Technol.* **2022**, *56*, 8167−8175.

(20) Bentel, M. J.; Yu, Y.; Xu, L.; Li, Z.; Wong, B. M.; Men, Y.; Liu, J. Defluorination of per- and polyfluoroalkyl substances (PFASs) with hydrated electrons: Structural dependence and implications to PFAS remediation and management. *Environ. Sci. Technol.* **2019**, *53*, 3718−3728.

(21) Su, Y.; Rao, U.; Khor, C. M.; Jensen, M. G.; Teesch, L. M.; Wong, B. M.; Cwiertny, D. M.; Jassby, D. Potential-driven electron transfer lowers the dissociation energy of the C-F bond and facilitates reductive defluorination of perfluorooctane sulfonate (PFOS). *ACS Appl. Mater. Interfaces* **2019**, *11*, 33913−33922.

(22) Rao, U.; Su, Y.; Khor, C. M.; Jung, B.; Ma, S.; Cwiertny, D. M.; Wong, B. M.; Jassby, D. Structural dependence of reductive defluorination of linear PFAS compounds in a UV/electrochemical system. *Environ. Sci. Technol.* **2020**, *54*, 10668−10677.

(23) Daily, R.; Minakata, D. Reactivities of hydrated electrons with organic compounds in aqueous-phase advanced reduction processes. *Environ. Sci.: Water Res. Technol.* **2022**, *8*, 543−574.

(24) Zhang, Y.; Moores, A.; Liu, J.; Ghoshal, S. New insights into the degradation mechanism of perfluorooctanoic acid by persulfate from density functional theory and experimental data. *Environ. Sci. Technol.* **2019**, *53*, 8672−8681.

(25) Hutter, J.; Iannuzzi, M.; Schiffmann, F.; VandeVondele, J. CP2K: Atomistic simulations of condensed matter systems. *WIREs Computational Molecular Science* **2014**, *4*, 15−25.

(26) Perdew, J. P.; Burke, K.; Ernzerhof, M. Generalized gradient approximation made simple. *Phys. Rev. Lett.* **1996**, *77*, 3865−3868.

(27) Larsen, R. E.; Glover, W. J.; Schwartz, B. J. Does the hydrated electron occupy a cavity? *Science* **2010**, *329*, 65−69.

(28) Devonshire, R.; Weiss, J. J. Nature of the transient species in the photochemistry of negative ions in aqueous solution. *J. Phys. Chem.* **1968**, *72*, 3815−3820.

(29) Barducci, A.; Bussi, G.; Parrinello, M. Well-tempered metadynamics: A smoothly converging and tunable free-energy method. *Phys. Rev. Lett.* **2008**, *100*, No. 020603.

(30) Biswas, S.; Wong, B. M. Ab initio metadynamics calculations reveal complex interfacial effects in acetic acid deprotonation dynamics. *J. Mol. Liq.* **2021**, *330*, No. 115624.

(31) Biswas, S.; Wong, B. M. High-temperature decomposition of diisopropyl methylphosphonate on alumina: Mechanistic predictions from ab initio molecular dynamics. *J. Phys. Chem. C* **2021**, *125*, 21922−21932.

(32) Biswas, S.; Kwon, H.; Barsanti, K. C.; Myllys, N.; Smith, J. N.; Wong, B. M. Ab initio metadynamics calculations of dimethylamine for probing pK_b variations in bulk vs. surface environments. *Phys. Chem. Chem. Phys.* **2020**, *22*, 26265−26277.

(33) Biswas, S.; Mallik, B. S. Proton transfer from water to anion: Free energy profile from first principles metadynamics simulations. *J. Mol. Liq.* **2016**, *219*, 810−814.

(34) Maza, W. A.; Breslin, V. M.; Owrutsky, J. C.; Pate, B. B.; Epshteyn, A. Nanosecond transient absorption of hydrated electrons and reduction of linear perfluoroalkyl acids and sulfonates. *Environ. Sci. Technol. Lett.* **2021**, *8*, 525−530.

(35) Digne, M.; Sautet, P.; Raybaud, P.; Euzen, P.; Toulhoat, H. Hydroxyl groups on γ-alumina surfaces: a DFT study. *J. Catal.* **2002**, *211*, 1−5.

(36) Digne, M.; Sautet, P.; Raybaud, P.; Euzen, P.; Toulhoat, H. Use of DFT to achieve a rational understanding of acid-basic properties of γ-alumina surfaces. *J. Catal.* **2004**, *226*, 54−68.

(37) Lian, C.; Ali, Z. A.; Kwon, H.; Wong, B. M. Indirect but efficient: Laser-excited electrons can drive ultrafast polarization switching in ferroelectric materials. *J. Phys. Chem. Lett.* **2019**, *10*, 3402−3407.

(38) Hanasaki, K.; Ali, Z. A.; Choi, M.; Del Ben, M.; Wong, B. M. Implementation of real-time TDDFT for periodic systems in the open-source PySCF software package. *J. Comput. Chem.* **2023**, *44*, 980−987.

(39) Ali, Z. A.; Yamijala, S. S.; Wong, B. M. A review of emerging photoinduced degradation methods for per- and polyfluoroalkyl substances in water. *Current Opinion in Chemical Engineering* **2023**, *41*, No. 100947.

(40) Mortensen, J. J.; Hansen, L. B.; Jacobsen, K. W. Real-space grid implementation of the projector augmented wave method. *Phys. Rev. B* **2005**, *71*, No. 035109.

(41) Filho, A. H. d. S.; de Souza, G. L. C. Examining the degradation of environmentally-daunting per- and poly-fluoroalkyl substances from a fundamental chemical perspective. *Phys. Chem. Chem. Phys.* **2020**, *22*, 17659−17667.

(42) Supercomputer Provides Catalyst for Cleaning Up Drinking Water Contaminants. *SDSC.* https://www.sdsc.edu/News%20Items/PR20211104_PFAS.html (accessed April 1, 2023).

(43) HPCWire 2022 Editors' Choice Awards - Best HPC Response to Societal Plight. *HPCWire.* https://www.hpcwire.com/2022-readers-editors-choice-societal-plight (accessed April 1, 2023).

(44) Oviedo, M. B.; Wong, B. M. Real-time quantum dynamics reveals complex, many-body interactions in solvated nanodroplets. *J. Chem. Theory Comput.* **2016**, *12*, 1862−1871.

(45) Ilawe, N. V.; Oviedo, M. B.; Wong, B. M. Real-time quantum dynamics of long-range electronic excitation transfer in plasmonic nanoantennas. *J. Chem. Theory Comput.* **2017**, *13*, 3442−3454.

(46) Ilawe, N. V.; Oviedo, M. B.; Wong, B. M. Effect of quantum tunneling on the efficiency of excitation energy transfer in plasmonic nanoparticle chain waveguides. *J. Mater. Chem. C* **2018**, *6*, 5857−5864.

(47) Yamijala, S. S.; Oviedo, M. B.; Wong, B. M. *Reviews in Computational Chemistry*, Vol. *32*; John Wiley & Sons, Ltd, 2022 Chapter 2, pp 45−79.

(48) Rodríguez-Borbón, J. M.; Kalantar, A.; Yamijala, S. S. R. K. C.; Oviedo, M. B.; Najjar, W.; Wong, B. M. Field programmable gate arrays for enhancing the speed and energy efficiency of quantum dynamics simulations. *J. Chem. Theory Comput.* **2020**, *16*, 2085−2098.

(49) Allec, S. I.; Sun, Y.; Sun, J.; Chang, C.-e. A.; Wong, B. M. Heterogeneous CPU+ GPU-enabled simulations for DFTB molecular dynamics of large chemical and biological systems. *J. Chem. Theory Comput.* **2019**, *15*, 2807−2815.

(50) Kumar, A.; Arantes, P. R.; Saha, A.; Palermo, G.; Wong, B. M. GPU-enhanced DFTB metadynamics for efficiently predicting free energies of biochemical systems. *Molecules* **2023**, *28*, 1277.

(51) Dieguez, A. P.; Choi, M.; Zhu, X.; Wong, B. M.; Ibrahim, K. Z. ML-based performance portability for time-dependent density functional theory in HPC environments. In *2022 IEEE/ACM International Workshop on Performance Modeling, Benchmarking and Simulation of High Performance Computer Systems (PMBS)*, 2022; pp 1−12.